Individually Addressable Gel−Integrated Voltammetric Microelectrode Array for High-Resolution Measurement of Concentration Profiles at Interfaces

ARTICLE *in* ANALYTICAL CHEMISTRY · JUNE 2001

Impact Factor: 5.64 · DOI: 10.1021/ac000615e · Source: PubMed

5 AUTHORS, INCLUDING:

Mary-Lou Tercier-Waeber
University of Geneva
68 PUBLICATIONS **1,633** CITATIONS

SEE PROFILE

Anal. Chem. **2001,** *73,* 2273−2281

Individually Addressable Gel-Integrated Voltammetric Microelectrode Array for High-Resolution Measurement of Concentration Profiles at Interfaces

Jianhong Pei,[†] Mary-Lou Tercier-Waeber,[†] Jacques Buffle,*[,†] Giovanni Carlo Fiaccabrino,[‡] and Milena Koudelka-Hep[‡]

CABE, Department of Inorganic, Analytical and Applied Chemistry, Science II, University of Geneva, 30 Quai E.-Ansermet, CH-1211 Geneva 4, Switzerland, and Institute of Microtechnology, University of Neuchâtel, Jacquet-Droz 1, 2007 Neuchâtel, Switzerland

The application of a novel voltammetric probe, based on an individually addressable gel-integrated microelectrode array (IA-GIME), for real-time, high-spatial resolution concentration profile measurements at interfaces is described. Reliability and validity of steep metal concentration gradients obtained with this novel system have been demonstrated by performing systematic tests at well-controlled liquid−liquid and liquid−solid interfaces. The liquid−liquid interface was formed by two layers of aqueous solutions with different components; only one layer contained trace metal ions (Pb(II) and Cd(II)); the individually addressable microelectrode array was placed at the interface of the liquid−liquid system; the concentration profiles were recorded as function of time; and the effective diffusion coefficients were calculated. The liquid−"solid" interface was formed from an aqueous solution layer overlying a bed of silica particles saturated with an aqueous solution. The sensor array has been used to monitor the diffusion processes of Tl(I) or Pb(II) from the liquid phase to the "solid" phase. The influences of porosity, geometry of the porous media, and complexation between metal ion and silica, on the diffusion processes, have been studied. All these results show that correct diffusion profiles of metal ions at interfaces can be obtained with 200-μm resolution with the IA-GIME. They also demonstrate that, for measurements in "solid" phase, the aforementioned factors must be considered carefully for correct calibration of any electrodes and the gel-integrated microelectrodes are unique tools to enable calibration of the sensors with synthetic solutions.

The biophysicochemical processes that influence the circulation of trace metals in natural aquatic systems are still ill-known due to their complexity. The highly variable nature of metal ion supply, mixing, and removal processes in lakes and oceans results in a great diversity of their distribution in the water column and sediments. Knowledge of their concentration profiles at the sediment−water interface is essential for understanding chemical and biological processes in sediment.[1−4] They are also required to understand the dynamic mechanisms of remobilization, solubility, and sorption and the exchange fluxes of solutes between sediment and the overlying water.[4−9] Since the chemical strata of sediment may be as thin as a few millimeters, measurements with high spatial resolution are a prerequisite to model biological, chemical, and physical processes and enable a clear understanding of the biogeochemical processes at sediment−water interface.

Techniques of diffusion gradients in thin films (DGT) and diffusion equilibration in thin films (DET) have been developed,[4,5,10−12] and are capable of providing concentration profiles in the pore waters at submillimeter resolution. These techniques can provide important information on the fluxes of species across the sediment−water interface. However, real-time measurements are not possible. Single voltammetric or amperometric microelectrodes, due to their high sensitivity, good selectivity, and small tip size, can fulfill the requirements of both high resolution and real-time measurements at constant depth. Steep concentration gradients

* To whom correspondence should be addressed. Telephone: 41-22-702-6431. Fax: 41-22-702-6069. E-mail: Jacques.Buffle@cabe.unige.ch.

[†] University of Geneva.

[‡] University of Neuchâtel.

(1) Stumm, W. *Chemistry of the Solid-Water Interface*; J. Wiley: New York, 1992.
(2) Hamilton-Taylor, J.; Davison W. In *Physics and Chemistry of Lakes*; Lerman, A., Ed.; Springer-Verlag, New York, 1995.
(3) Santschi, P.; Hohener, P.; Benoit, G.; Buchholtz-ten-Brink, M. *Mar. Chem.* **1990**, *30*, 269.
(4) Zhang, H.; Davison, W.; Miller. S.; Tych, W. *Geochim. Cosmochim. Acta* **1995**, *59*, 4181.
(5) Zhang, H.; Davison, W. *Anal. Chem.* **1995**, *67*, 3391.
(6) Gobeil, C.; Macdonald, R. W.; Smith, J. N. *Environ. Sci. Technol.* **1999**, *33*, 4194.
(7) Aller, R. C. *Geochim. Cosmochim. Acta* **1988**, *52*, 751.
(8) Tessier, A. In *Environmental Particles*; Buffle, J., van Leeuwen, H. P., Eds.; Lewis: Boca Raton, FL, 1992; Vol. 1.
(9) Belzile, N.; DeVitre, R. R.; Tessier, A. *Nature* **1989**, *340*, 376.
(10) Davison, W.; Zhang, H.; Grime, G. W. *Environ. Sci. Technol.* **1994**, *28*, 1623.
(11) Shuttleworth, S. M.; Davison, W.; Hamilton-Taylor, J. *Environ. Sci. Technol.* **1999**, *33*, 4169.
(12) Davison, W.; Fones, G. R.; Grime, G. W. *Nature* **1997**, *387*, 885.

10.1021/ac000615e CCC: $20.00
Published on Web 04/14/2001

of O_2,[13−15] nitrate,[16] ammonia,[17] and Fe(II), Mn(II), S(−II), O_2[18,19] have been at the sediment−water interface with microelectrodes. In fact, the introduction of microelectrodes in aquatic ecology has significantly improved the understanding of microbial processes at aquatic interfaces.[14,20] But a single electrode can only measure concentration at one depth at a time, and recording a full concentration profile may take hours. In addition, the sediment may be perturbed at each intrusion step of the microelectrode and full reequilibration may take hours. These problems can be overcome or minimized by using individually addressable microelectrode arrays with which measurement at all depths is performed simultaneously in real time. A high spatial resolution can be realized by using the appropriate geometry of the sensor array. Recently, the development of an individually addressable microelectrode array has received much attention and represents a challenging work due to the sophisticated demands on technology. The conventional way to individually address each electrode of an array is to connect the electrode line to a corresponding bond pad.[21,22] The electrochemical measurements are then carried out on each electrode sequentially, not simultaneously. This approach is easier from a technical viewpoint. Under such condition, however, the recording of a whole concentration profile is long; e.g., typically 3 h was required for recording complete cyclic voltammograms on a 64-individually addressable microelectrode array.[23] Simultaneous current measurements on chip have been reported on an individually addressable microelectrode array, by using an integrated circuit (IC).[24,25] Chromatographic and biomedical applications of such individually addressable microsensor arrays have been reported.[26−29] But only amperometric, not voltammetric measurements have been done with these sensors, and sequential multichannel detection systems were used.

Recently we developed a voltammetric sensor and probe allowing real-time, high spatial resolution measurements of the whole concentration profile of trace elements.[30] The heart of this system is an individually addressable gel-integrated Hg-plated Ir-based microelectrode array (IA-GIME) with 64 individually addressable lines, built using the same technology as that used for the iridium-based interconnected microelectrode array, reported in refs 31−33. The voltammetric probe is based on a powerful double multiplexing system and a single potentiostat. The hardware and firmware were designed to allow quasi-simultaneous measurements over the 64 individually addressable microsensor lines (i.e., deposition step in ASV technique is done simultaneously on all electrodes, and the stripping step is performed sequentially but with a maximum time delay of 35 μs between measurements on the various lines) (see ref 30 for details). This was the first system reported allowing simultaneous recording of complete voltammograms for a large number of individually addressable microelectrodes with fast dynamic techniques such as square wave anodic stripping voltammetry (SWASV). This paper reports the application of this probe for real-time metal ion concentration profile measurements as a function of time, at well-controlled liquid−liquid and liquid−"solid" interfaces. The liquid−liquid interface was formed by two layers of aqueous solutions with different compositions. The liquid−"solid" interface was formed by an aqueous solution layer overlaying a bed of silica particles saturated with an aqueous solution. The effective diffusion coefficients of metal ions were calculated by fitting experimental data from the concentration profiles with theoretical analytical equations and compared to literature values. Three well-controlled systems were studied: (i) the diffusion of uncomplexed Tl(I) at the liquid−"solid" interface to test the influences of porosity and tortuosity of the "solid" medium in noncomplexing conditions; (ii) the diffusion of Pb(II) at the liquid−"solid" interface to test the additional effect of Pb(II) complexation by silica particles; (iii) the diffusion of Pb(II) and Cd(II) at the liquid−liquid interface to test the role of microconvection at the interface. Such tests performed under well-controlled conditions are required to correctly interpret experimental data obtained in a complex real sediment−water interface. They also showed that gel-integrated microelectrodes are required to enable calibration of the measured currents in terms of concentration, based on synthetic solutions.

EXPERIMENTAL SECTION

Chemicals. All reagents used, except $Hg(CH_3COO)_2$ and KSCN (analytical grade), were Suprapur-grade. The LGL agarose used to cover the IA-GIME (maximum sulfur, 0.3%; gel strength at 1.5%, 2000 g cm^{-2}) was purchased from Biofinex. Silica gel 100 (diameter, 0.2−0.5 mm) used as solid phase was obtained from Fluka. Stock solutions of Cd(II), Pb(II), Tl(I) (concentration of 1 g L^{-1}) (pH 2), Titrisol, 1 M HNO_3, and 1 M NaOH were purchased from Merck. All solutions were freshly prepared before use by dilution in Milli-Q water. All the experiments were carried out at room temperature.

Instrumentation and Experimental Conditions. An interconnected gel-integrated Hg-plated Ir-based microelectrode ar-

(13) Revsbech, N. P.; Jørgensen, B. B.; Blackburn, T. H. *Science* **1980**, *207*, 1355.
(14) Reimers, C. E, Fischer, K. M.; Merewether, R.; Smith, K. L., Jr.; Jahnke, R. A. *Nature* **1986**, *320*, 24.
(15) Nielsen, L. P.; Christensen, P. B.; Revsbech, N. P. *Microb. Ecol.* **1990**, *19*, 63.
(16) Sweerts, J. R. A.; de Beer, D. *Appl. Environ. Microbiol.* **1989**, *55*, 754.
(17) de Beer, D.; Van den Heuvel, J. C. *Talanta* **1988**, *35*, 728.
(18) Brendel, P. J.; Luther, G. W., III. *Environ. Sci. Technol.* **1995**, *29*, 751.
(19) Luther, G. W., III; Brendel, P. J.; Lewis, B. L.; Sundby, B.; Lefrançois. L.; Silverberg. N.; Nuzzio, D. B. *Limnol. Oceanogr.* **1998**, *43*, 325.
(20) Revsbech, N. P.; Sorensen, J.; Blackburn, T. H. *Limnol. Oceanogr.* **1980**, *25*, 403.
(21) Deer, D. W.; Tobias, C. W. *J. Electrochem. Soc.* **1987**, *134*, 369.
(22) Connolly, P.; Moores, G. R.; Monaghan, W.; Shen, J.; Britland, S.; Clark, P. *Sens. Actuators* **1992**, *B6*, 113.
(23) Sullivan, M. G.; Utomo, H.; Fagan, P. J.; Ward, M. D. *Anal. Chem.* **1999**, *71*, 4369.
(24) Meyer, H.; Drewer. H.; Gründig, B.; Cammann, K.; Kakerow, R.; Manoli, Y.; Mokwa, W.; Rospert, M. *Anal. Chem.*, **1995**, *67*, 1164.
(25) Fiaccabrino, G. C.; Koudelka-Hep, M.; Jeanneret, S.; van den Berg, A.; de Rooij, N. F. *Sens. Actuators* **1994**, *B19*, 675.
(26) Matson, W. R.; Gamache, P. H.; Beal, M. F.; Bird, E. D. *Life Sci.* **1987**, *41*, 905.
(27) Hoogvliet, J. C.; Reijn, J. M.; van Bennekom, W. P. *Anal. Chem.* **1991**, *63*, 2418.
(28) Aoki, A.; Matsue, T.; Uchida, I. *Anal. Chem.* **1992**, *64*, 44.
(29) Hinkers, H.; Hermes, T.; Sundermeier, C.; Borchardt, M.; Dumsehat, C.; Bücher, S.; Bühner, M.; Camman, K.; Knoll, M. *Sens. Actuators* **1995**, *B24−25*, 300.
(30) Tercier-Waeber, M.-L.; Pei, J.; Buffle, J.; Fiaccabrino, G. C.; Koudelka-Hep, M.; Riccardi, G.; Confalonieri, F.; Sina, A.; Graziottin, F.; *Electroanalysis* **2000**, *12*, 27.
(31) Belmont-Hebert, C.; Tercier, M. L.; Buffle, J.; Fiaccabrino, G. C.; de Rooij, N. F.; Koudelka-Hep, M. *Anal. Chem.* **1998**, *70*, 2949.
(32) Tercier-Waeber, M.-L.; Belmont-Hebert, C.; Buffle, J. *Environ. Sci. Technol.* **1998**, *32*, 1515.
(33) Pei, J.; Tercier-Waeber, M.-L.; Buffle, J. *Anal. Chem.* **2000**, *72*, 161.

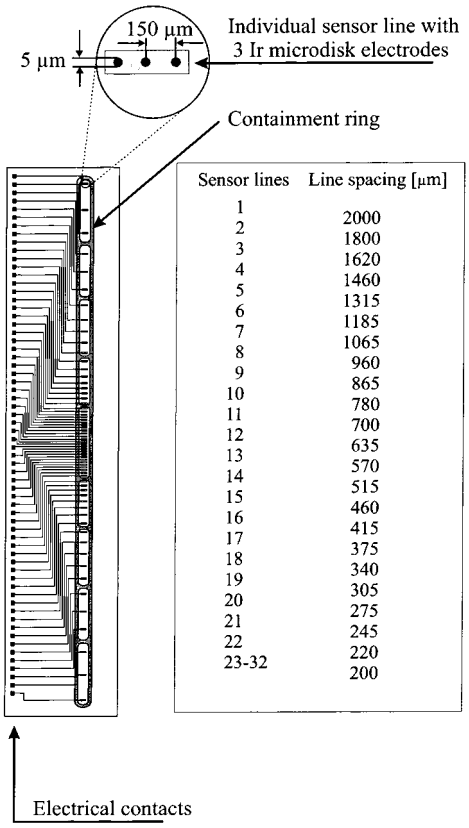

Figure 1. Schematic diagram of the individually addressable Ir-based microelectrode array (IA-GIME).

ray,[31] connected to a computer-controlled Amel 433A polarograph, was used to study the complexation between metal ions and silica particles. The recently developed voltammetric probe described in detail in ref 30 was used to perform real-time metal ion concentration profile measurements as a function of time at well-controlled interfaces. The heart of the probe is an individually addressable gel-integrated Hg-plated Ir-based microelectrode array (Figure 1). Details of the fabrication and characteristics of this microsensor are reported in ref 30 and only briefly summarized here. It is made by using thin film and photolithographic techniques. It consists of 64 lines of three Ir microdisk electrodes of 5 μm in diameter and a horizontal center-to-center spacing of 150 μm. The spacing between the electrode lines 1−23 decreases from 2000 to 220 μm and then stays at a constant value of 200 μm between sensor lines 23−32 (Figure 1). The geometry of the sensor lines 33−64 is a mirror image of that for the lines 1−32. The sensor lines are surrounded by a 300-μm-thick EPON Su-8 containment ring for the gel. Both sensors (i.e., the interconnected and the individually addressable microelectrode array) were covered with a 1.5% LGL agarose antifouling membrane. More details on the gel characteristics, preparation, and features are given in refs 31−35. A Metrohm Ag/AgCl/3 M KCl//1 M $NaNO_3$ reference electrode and a platinum rod counter electrode were used in both systems. Mercury semidrops were deposited through the gel layer onto the Ir substrate at −400 mV in a N_2 deoxygenated 5 mM $Hg(CH_3COO)_2$ and 10^{-2} M $HClO_4$ solution before each set of experiments. Reoxidation of the mercury was also carried out through the agarose by scanning the potential linearly from −300 to 300 mV, at 5 mV/s, in a N_2 degassed 1 M KSCN solution after experiments.[31,34] SWASV working conditions were as follows: deposition potential, −1000 mV; deposition time, 1 min; final potential, −100 mV; pulse amplitude, 25 mV; step amplitude, 4 mV (new voltammetric probe); 8 mV (Amel potentiostat); frequency, 100 Hz (new voltammetric probe); 50 Hz (Amel potentiostat); precleaning potential, −100 mV; precleaning time, 15 s. The cleaning step, applied before each measurement, ensures uniform spreading of the mercury layer on the iridium surface and complete removal of the elements preconcentrated in the mercury film during the previous measurement.[34] A pH meter (model 744, Metrohm) was used to measure pH values. A conductivity meter (D-812, Weilheim) was used to measure the electrical resistivities in both the upper solution phase and the silica "solid" phase at the liquid−"solid" system.

For the study of complexation between trace metal and solid phase, the pHs were fixed at various values from 2 to 7.5 as follows: in the pH range 2−3.5 by using HNO_3; in the pH range 3.5−5 by 0.01 M Suprapur acetate buffer solutions; in the pH range 5.5−7.5 by 0.01 M analytical-grade 2-(*N*-morpholino)ethanesulfonic acid (MES) buffer solutions. It was found that less than 5% of Pb(II) is complexed by these buffers under the experimental conditions used. Thus, all the desorbed Pb(II) can be considered as free Pb^{2+}.

Preparation of Liquid−Liquid Interface. The best way to prepare a well-controlled liquid−liquid interface was studied by using a Crystal violet-containing solution and water as colorless solution. In both cases, $NaNO_3$ salt was used as electrolyte and to adjust the solution density. It was found to be impossible to add one solution onto the other, slightly denser one, without (even small) interfacial mixing. On the other hand, a well-defined interface can be obtained when the bottom solution is introduced below the upper one and the interface is slowly pushed upward. For diffusion measurements, the compositions of the two aqueous solutions were as follows: 0.01 M $NaNO_3$ + 0.01 M acetate buffer solution (pH 4.5) for the top solution and 5 μM both Pb(II) and Cd(II) in 0.25 M $NaNO_3$ + 0.01 M acetate buffer solution (pH 4.5) for the bottom solution. The top solution (100 mL) was first introduced into a Plexiglas cylindrical measurement cell and the bottom half of the IA-GIME was inserted into the solution. Then the bottom solution (~100 mL) was slowly introduced into the bottom of the cell, via a pipet, using a carefully controlled release rate achieved by a pinchcock attached to the robber bulb of the pipet. Typically, a slow flow rate of 0.75 mL/min was used to minimize the turbulences. The small difference of density, due to the different concentrations, is helpful to minimize disturbance. Introduction of the bottom solution was stopped when the middle of the sensor array was close to the interface. To minimize turbulences, the measurement cell was fixed on a special antivibration table (for high accuracy analytical balance) and the temperature was kept constant at 24 ± 1 °C.

Preparation of Liquid−"Solid" Interface. The liquid−"solid" interface was prepared as follows: 50 g of silica was first equilibrated with 500 mL 0.1 M $NaNO_3$ + 0.01 M acetate buffer solution (pH 4.65) under magnetic stirring for 2 days and the IA-GIME was then positioned vertically at the liquid−"solid" interface,

(34) Tercier, M.-L.; Buffle, J. *Anal. Chem.* **1996**, *68*, 3670.
(35) Tercier, M. L.; Buffle, J.; Graziottin, F. *Electroanalysis* **1998**, *10*, 355.

in such a way that half of the sensor was in the "solid" phase. The IA-GIME was well fixed in the cell, and the cell was fixed on the special antivibration table. A given concentration of Tl(I) or Pb(II) was added to the top solution and then nitrogen gas was used to gently bubble the top solution for homogenization. This process should be very carefully controlled to avoid disturbance at the interface. The reliability of the preparation of the well-controlled liquid−"solid" interface was checked by adding Crystal violet or $K_3Fe(CN)_6$ as dyes to the top solution. Under optimum condition, a steep concentration gradient of solute is formed at the liquid−"solid" interface and real-time evolution of concentration profile can be measured.

Calibration of the IA-GIME. The correct functioning of IA-GIME was first checked in a standard metal ion solution before making profile measurements. Systematic calibrations were also performed after the profile measurements. The calibration curves were determined in N_2 degassed 0.1 M $NaNO_3$ + 0.01 M acetate buffer (pH 4.65) solution spiked with metal ions in the concentration range 1×10^{-7}−5×10^{-6} M (six points). Linear relationships between peak currents and concentrations were obtained at each sensor line ($R \geq 0.998$) and were used to compute the concentration profiles.

RESULTS AND DISCUSSION

Tl(I) Diffusion at the Liquid−"Solid" Interface. Typical concentration profiles of Tl(I) and their variation as function of time at the liquid−"solid" interface are shown in Figure 2a. Tl(I) was first selected for measurements of concentration profiles, because Tl(I)/Tl(0) is a reversible redox system at Hg film electrode surface and Tl(I) is not complexed by silica. This was checked by SWASV measurements of Tl(I) in silica suspensions using an interconnected microelectrode array. Thus, the concentration profiles at the liquid−"solid" interface are mainly controlled by the diffusion process. Even in the absence of complexation, the effective diffusion coefficient of a metal ion in a porous medium is different from that in the free solution, as the flux is also related to the physical characteristics of the medium, i.e., the porosity and the geometric tortuosity of pores,[36−39] according to eq 1, when there is no accumulation of the diffusing species at the interface:

$$D_w\left(\frac{\partial C_w(x,t)}{\partial x}\right)_{x=0} = \phi\theta^{-2}D_w\left(\frac{\partial C_s(x,t)}{\partial x}\right)_{x=0} \quad (1)$$

with

$$\phi\theta^{-2}D_w = D_s^{\text{eff}} \quad (1a)$$

where the subscripts w and s refer to water (i.e., liquid phase) and "solid" phase, respectively; $C(x,t)$ is the analyte concentration at depth x ($x > 0$ in solution phase and $x < 0$ in "solid" phase) and time t; D_s^{eff} is the effective diffusion coefficient in the "solid" phase; ϕ is the porosity of the "solid" phase, defined as the ratio of porewater volume over total volume of "solid" phase and is equal to 0.85 ± 0.04 in our system; and θ is the geometric tortuosity of the porous media.[36−39] In practice, θ cannot be measured directly; however, the hindrances of electrical conductance and diffusion of solute in porous media are analogous in many ways. It is thus possible to derive an indirect relationship between θ and the electrical resistivity of the porous medium.[36,39] The formation resistivity factor, F, is defined as $F = R_s/R_w$, where R_s is the resistivity of the "solid" phase and R_w the resistivity of the interstitial fluid in absence of the solid. The relation between F and the tortuosity depends on the geometric model used to describe the porespace, but generally it is accepted as $\theta^2 = \phi F$,[36−39] provided the conductance due to the interstitial fluid is much larger than that of the solid. This condition was satisfied in our system due to the high concentration of supporting electrolyte, and a value of $F = 1.36 \pm 0.05$ was obtained experimentally. Equation 1a can thus be rewritten as $D_s^{\text{eff}} = D_w/F$.

The time evolution of the complete concentration profile can be obtained by applying Fick's second law to semi-infinite liquid and "solid" phases, with eq 1 as a boundary condition. The analytical expressions of the concentration profiles are then given by eqs 2 and 3 for the liquid and "solid" phases, respectively:[40]

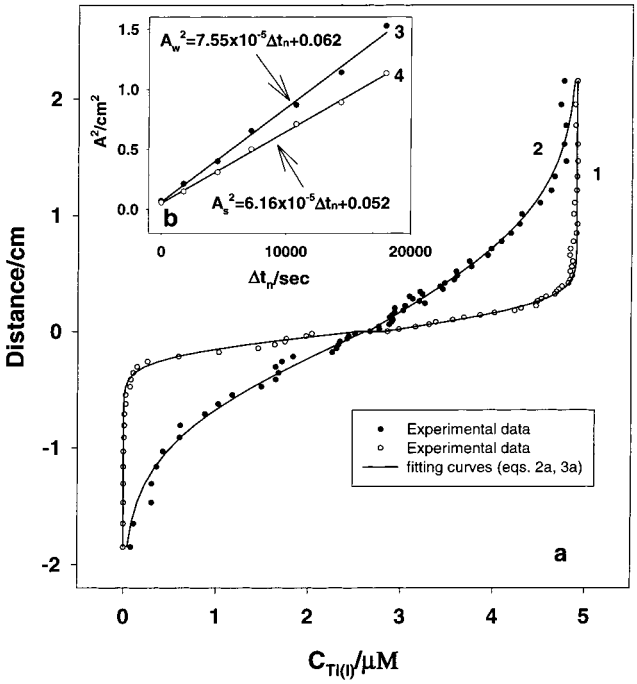

Figure 2. (a), Typical Tl(I) concentration gradients measured by SWASV at the liquid−"solid" interface using the IA-GIME: (1) first measurement ($t = t_1$); (2) measurement after 5 h ($t = t_1 + 5$ h). Inset b, the linear relationship obtained between A^2 and Δt_n in (3) the liquid phase and (4) the "solid" phase. Composition of the liquid phase: 4.9 μM Tl(I) + 0.1 M $NaNO_3$ + 0.01 M acetate buffer solution (pH 4.65); composition of the "solid" phase, 0.1 M $NaNO_3$ + 0.01 M acetate buffer (pH 4.65) + silica particles. SWASV conditions used: precleaning $E = -100$ mV and $t = 15$ s; deposition $E = -1000$ mV and $t = 60$ s; final $E = -100$ mV; pulse amplitude, 4 mV; frequency, 100 Hz. Positive and negative distances are related to liquid and "solid" phases, respectively.

(36) Glud, R. N.; Jensen, K.; Revsbech, N. P. *Geochim. Cosmochim. Acta* **1995**, *59*, 231.
(37) Ullman, W.; Aller, R. C. *Limnol. Oceanogr.* **1982**, *27*, 552.
(38) Li, Y.-H.; Gregory, W. *Geochim. Cosmochim. Acta* **1974**, *38*, 703.
(39) Iversen, N.; Jørgensen, B. B. *Geochim. Cosmochim. Acta* **1993**, *75*, 571.
(40) Crank, J. *The Mathematics of Diffusion*; Oxford University Press: New York, 1975.

$$C_w(x,t) = \frac{C_o}{1+\sqrt{D_s^{eff}/D_w}}\left[1+\sqrt{D_s^{eff}/D_w}\ \mathrm{erfc}\frac{x}{2\sqrt{D_w t}}\right] \quad (2)$$

$$C_s(x,t) = \frac{C_0}{1+\sqrt{D_s^{eff}/D_w}}\ \mathrm{erfc}\frac{|x|}{2\sqrt{D_s^{eff} t}} \quad (3)$$

where C_0 is the initial concentration of the analyte in the top solution phase; $C_w(x,t)$ and $C_s(x,t)$ are the concentrations of the analyte at time t and distance x in the liquid and "solid" phases, respectively. In practice, the experimental data are fitted using eqs 2 and 3 rewritten as eq 2a and eq 3a.

$$C_w(x,t) = \frac{C_0}{1+B}\left[1+B^*\ \mathrm{erfc}\ \frac{x}{A_w}\right] \quad (2a)$$

$$C_s(x,t) = \frac{C_0}{1+B}\ \mathrm{erfc}\frac{|x|}{A_s} \quad (32)$$

where $B = (D_s^{eff}/D_w)^{1/2}$; $A_w = 2(D_w(t_1 + \Delta t_n))^{1/2}$ for the liquid and $A_s = 2(D_s^{eff}(t_1 + \Delta t_n))^{1/2}$ for the "solid" phases; t_1 is the measurement time of the first concentration profile and Δt_n is the time interval between the measurements of the first and the nth concentration profile. The time t was expressed as $t_1 + \Delta t_n$ as t_1 is not precisely known under our conditions. It was thus used as a fitting parameter as well as D. D_w and D_s^{eff} have the same meaning as in eq 1. The values of A_w, A_s, and B obtained by curve fitting using Matlab are shown in Table 1. As expected, B values are close to each other for all the concentration profiles. Even though the values for "solid" phase are slightly larger than those for liquid phase, the difference is within experimental error. From the average value of $B = 0.872$, $D_w/D_s^{eff} = 1/B^2 = 1.31$ is computed. This value is in good agreement with the experimental value of $F = 1.36 = D_w/D_s^{eff}$ obtained from conductivity measurements (see above). An empirical relationship between the formation resistivity factor F and the porosity ϕ has been suggested for natural sediments: $F = 1/\phi^m$.[36,39] The parameter m is a constant specific for the sediment nature, i.e., $m = 1.3-2$ for sand and $m = 2.5-5.4$ for clay particles.[36−39] From the values of $F = 1.31$ and $\phi = 0.85$ determined for our system, we get $m = 1.66$. It is in the range of the sand sediment constant, which is coherent for silica particles. By imposing the average value of $B = 0.872$ for both the liquid and "solid" phases, in the curve fitting of experimental data of Figure 2a using eqs 2a and 3a, other sets of A_w and A_s values are obtained and shown in Table 1. A_w^2 and A_s^2 are plotted versus Δt_n in Figure 2b (curves 3 and 4) giving linear relationships. The slope of curve 3, combined with $B = 0.872$, gives $D_w = (1.89 \pm 0.06) \times 10^{-9}$ m^2 s^{-1} and $D_s^{eff} = (1.44 \pm 0.22) \times 10^{-9}$ m^2 s^{-1}, while that of curve 4 gives $D_w = (2.02 \pm 0.20) \times 10^{-9}$ m^2 s^{-1} and $D_s^{eff} = (1.54 \pm 0.03) \times 10^{-9}$ m^2 s^{-1}. These values are in agreement with each other and D_w is very close to the literature value $D_w = 1.99 \times 10^{-9}$ m^2 s^{-1}.[41] These results thus validate the use of IA-GIME for accurate concentration profile measurements at liquid−"solid" interface in noncomplexing medium.

Pb(II) Diffusion at the Liquid−"Solid" Interface. The diffusion of Pb(II) at the liquid−"solid" interface using silica particles as the "solid" phase has been investigated to check the role of metal complexation by the solid particles on the diffusion process.

Table 1. Parameters Obtained from the Theoretical Fitting of the Experimental Concentration Profiles of Tl(I) at the Liquid−"Solid" Interface[a]

	Liquid Phase		
Δt (min)	B	A_w[b]	A_w[c]
0	0.741	0.286	0.264
30	0.835	0.464	0.454
75	0.830	0.640	0.621
120	0.870	0.795	0.794
180	0.848	0.932	0.914
240	0.841	1.073	1.046
300	0.851	1.229	1.208
	"Solid" Phase		
Δt (min)	B	A_s[b]	A_s[c]
0	0.927	0.251	0.243
30	0.956	0.410	0.391
75	0.907	0.577	0.565
120	0.936	0.749	0.720
180	0.878	0.861	0.858
240	0.912	0.985	0.960
300	0.877	1.086	1.083

[a] Average value and standard deviation of B are 0.872 and 5.3%, respectively. [b] Results obtained by curve fitting using B and A_w or A_s as fitting parameters. [c] Result obtained by using a constant average B value and A_w or A_s as fitting parameters.

The effect of pH on the complexation of Pb(II) by SiO_2 (0.1 kg/L) surface was studied in a solution of 20 mL of 0.1 M $NaNO_3$ and 2×10^{-7} M Pb(II) at various pH. The pH was adjusted in the range of 2−7.5 by different buffers as described in the Experimental Section. Pb(II) was left to equilibrate in these suspensions under magnetic stirring for 48 h. Then SWASV measurements were carried out with an interconnected gel-integrated Hg-plated Ir-based microelectrode array and the ratio between the free Pb-(II) and the total Pb(II) concentration ($[Pb^{2+}]/[Pb(II)]_t$) was computed (Figure 3).

The complexation reaction of Pb(II) with the silanol groups of SiO_2 can be approximated by a competition reaction with H^+ and formation of both monodentate or bidentate surface complexes:[42−46]

$$\equiv SiOH + Pb^{2+} \leftrightarrow \equiv SiOPb^+ + H^+ \quad (4)$$

$$2\equiv SiOH + Pb^{2+} \leftrightarrow (\equiv SiO)_2Pb + 2H^+ \quad (5)$$

The relative importance of monodentate and bidentate complexes can be assessed of the plot $\log([Pb(II)]_{ad}/[Pb^{2+}])$ versus pH in (Figure 3),[33] the region of the pH jump in Figure 3,[33] where $[Pb^{2+}]$ and $[Pb(II)]_{ad}$ are the molar concentrations of free and adsorbed

(41) David, R. L. *Handbook of Chemistry and Physics*, 75th ed.; CRC Press: Boca Raton, FL, 1994; pp 5−90,

(42) Wang, Z.-j.; Stumm, W. *Neth. J. Agric. Sci*. **1976**, *55*, 281.

(43) Kurbatov, M. H.; Wood, G. B.; Kurbatov, J. D. *J. Phys. Chem*. **1951**, *55*, 1170.

(44) Hohl, H.; Stumm, W. *J. Colloid Interface Sci*. **1976**, *55*, 281.

(45) Schindler, P. W.; Fürst, B.; Dick, R.; Wolf, P. U. *J. Colloid Interface Sci*. **1976**, *55*, 469.

(46) Hachiya, K.; Sasaki, M.; Saruta, Y.; Mikami, N.; Yasunaga, T. *J. Phys. Chem*. **1984**, *88*, 23.

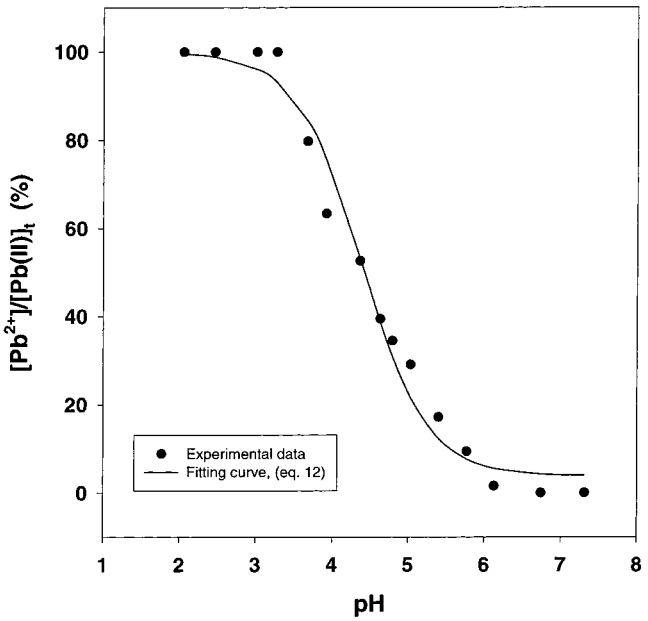

Figure 3. Effect of pH on the complexation of Pb(II) by SiO_2 suspension (0.1 kg/L) in 0.1 M $NaNO_3$ and 2×10^{-7} M Pb(II). The samples were equilibrated for more than 48 h at each pH. SWASV conditions used: precleaning $E = -100$ mV and $t = 15$ s; deposition $E = -1000$ mV and $t = 1$ min; final $E = -100$ mV; pulse amplitude, 8 mV; frequency, 50 Hz. Full line is the theoretic curve, computed from eq 12.

Pb ions, respectively. The slope of this curve is equal to the number of protons released during the complexation reaction. Under our experimental conditions, the slope was 0.86 ± 0.05, showing that only reaction 4 occurs.

This reaction is thus rewritten more rigorously by combining the two reactions 6 and 7:

$$\equiv SiO^- + H^+ \leftrightarrow \equiv SiOH \tag{6}$$

and

$$\equiv SiO^- + Pb^{2+} \leftrightarrow \equiv SiOPb^+ \tag{7}$$

The corresponding equilibrium constants are the following:

$$K_H = \frac{[\equiv SiOH]}{[\equiv SiO^-][H^+]} \tag{8}$$

and

$$\beta_{Pb} = \frac{[\equiv SiOPb^+]}{[Pb^{2+}][SiO^-]} \tag{9}$$

The following mass balance equations are also applicable

$$[S]_t = [\equiv SiOH] + [\equiv SiO^-] + [\equiv SiOPb^+] \tag{10}$$

$$[Pb(II)]_t = [Pb^{2+}] + [\equiv SiOPb^+] \tag{11}$$

where $[S]_t$ is the total complexing site concentration of the silica particles. In our case, $[\equiv SiOPb^+] \ll [S]_t$, so that eq 12 can be combining with eqs 8−11, to get

$$\frac{[Pb^{2+}]}{[Pb(II)]_t} = \frac{K_H[H^+] + 1}{\beta_{Pb}[S]_t + K_H[H^+] + 1} \tag{12}$$

Equation 12 was used to fit the experimental data of Figure 3 (full line), and a good agreement is found between the experimental data and the theoretical curve. The following parameters were thus obtained: $\beta_{Pb}[S]_t = 25.2 \pm 0.7$ and $K_H = (6.33 \pm 0.76) \times 10^5$ M^{-1}. In addition, $[S]_t$ was determined experimentally by first adding an excess of standard base solution to a dispersion of SiO_2 (0.1 kg/L) and equilibrating the suspension for 2 days. After centrifugation, the excess base in the supernatant was back-titrated with standard acid.[44−46] A value of $[S]_t = 1.38$ mol kg^{-1} SiO_2 was thus obtained, corresponding to a molar concentration of $[S]_t = 0.138$ M. Combining this value with that of $\beta_{Pb}[S]_t$ obtained above gives a β_{Pb} value of 1.83×10^2 M^{-1}.

The measurements of Pb(II) diffusion at the liquid−"solid" interface were carried out similarly to those for Tl(I) as described in the Experimental Section. The concentration of Pb(II) added to the top solution was 5 μM. However, SWASV measurements in the top solution showed that the free Pb^{2+} concentration in solution was only 4.1 μM. This results from the partial complexation of Pb(II) by some small size colloidal silica left in suspension in the top solution after preparation of the interface. Due to the selectivity of IA-GIME, only the peak current of free Pb(II) is measured. Indeed the diffusion coefficient of those colloidal complexes is much smaller than that of free Pb(II), and moreover, colloids are excluded from the agarose gel of IA-GIME.[32] Thus, the contribution of colloidal Pb(II) to the current, and consequently the concentration profiles, measured by IA-GIME can be ignored. The initial concentration of Pb(II) was then taken as 4.1 μM instead of 5 μM. Examples of typical concentration profiles of Pb(II) and their change with time at this interface are shown in Figure 4a, curves 1 and 2.

Due to the complexation between Pb(II) and silica particles, the effective diffusion coefficient of Pb(II) in the "solid" phase depends on its surface complexation (adsorption) by silica particles. Assuming fast adsorption equilibrium compared to the diffusion process, eq 13 can be used to express the influence of adsorption reaction on the average diffusion coefficient, $\bar{D}_p$ in the pore solution:[47]

$$\bar{D}_p = D_w\frac{[Pb^{2+}]}{[Pb(II)]_t} + D_{ad}\frac{[Pb(II)]_{ad}}{[Pb(II)]_t} \tag{13}$$

where D_{ad} and $[Pb(II)]_{ad}$ are the diffusion coefficient and the concentration of Pb(II) bound to silica particles, respectively. Note that $\bar{D}_p$ does not take into account the porosity and tortuosity effects discussed above. The general equation for the effective diffusion coefficient of Pb(II) in the "solid" phase is thus obtained

(47) Heyrovsky, J.; Kuta, J. *Principles of Polarography*; Publishing House of the Czechoslovak Academy of Science: Prague, 1968.

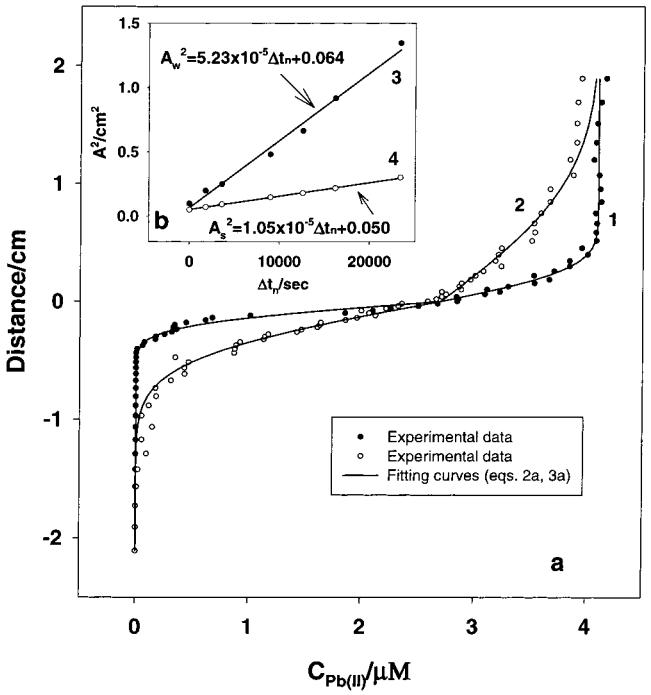

Figure 4. (a) Typical Pb(II) concentration gradients measured by SWASV at a liquid−"solid" interface using the IA-GIME: (1) first measurement ($t = t_1$); (2) measurement after 6.5 h ($t = t_1 + 6.5$ h). Inset b, the linear relationship obtained between A^2 and Δt_n in (3) the liquid phase and (4) the "solid" phase. Top liquid solution, 4.1 μM Pb(II) + 0.1 M $NaNO_3$ + 0.01 M acetate buffer solution (pH 4.65); bottom "solid" phase, 0.1 M $NaNO_3$ + 0.01 M acetate buffer (pH 4.65) + silica particles. SWASV conditions used as in Figure 2. Positive and negative distances are related to liquid and "solid" phases, respectively.

by replacing D_w in eq 1a by $\bar{D}_p$ of eq 13;

$$D_s^{eff} = \left(D_w \frac{[Pb^{2+}]}{[Pb(II)]_t} + D_{ad} \frac{[Pb(II)]_{ad}}{[Pb(II)]_t} \right) \theta^{-2} \phi \qquad (14)$$

Rigorously, the term $\phi\theta^{-2}$ may be different (smaller) for colloidal Pb complexes than for free Pb ion, but because $D_{ad} \ll D_w$, and $[Pb^{2+}]/[Pb]_t \sim 0.4$ under our operating conditions (see Figure 4 and eq 12), the term corresponding to the adsorbed Pb is anyway much smaller than that corresponding to the free Pb^{2+} and can be ignored. Thus, eq 14 can be simplified as eq 15.

$$D_s^{eff} \cong D_w \phi \theta^{-2} \frac{[Pb^{2+}]}{[Pb(II)]_t} \cong \frac{D_w\ [Pb^{2+}]}{F\ [Pb(II)]_t} \qquad (15)$$

The concentration gradient of Pb(II) can be calculated by combining Fick's second law with the boundary condition given by eq 1. Equations 2, 3, 2a, and 3a are still usable for curve fitting, except that D_s^{eff} is now given by eq 15. Values of B, A_s, and A_w were obtained from experimental data both in the liquid phase using eq 2a and in the "solid" phase using eq 3a (Table 2). As for Tl(I), similar B values were obtained in both cases (standard deviation is 4.7%), indicating a well-defined interface. By performing the curve fitting with the average value $B = 0.519$, the values of A_w and A_s in the liquid and "solid" phases were also obtained

Table 2. Parameters Obtained from the Theoretical Fitting of the Experimental Concentration Profiles of Pb(II) at the Liquid−"Solid" Interface[a]

	Liquid Phase		
Δt (min)	B	A_w[b]	A_w[c]
0	0.468	0.337	0.312
30	0.524	0.441	0.444
60	0.516	0.499	0.496
150	0.516	0.696	0.693
210	0.538	0.790	0.814
270	0.542	0.921	0.956
390	0.527	1.142	1.158
	"Solid" Phase		
Δt (min)	B	A_s[b]	A_s[c]
0	0.424	0.211	0.222
30	0.434	0.253	0.265
60	0.509	0.301	0.303
150	0.542	0.389	0.383
210	0.566	0.437	0.424
270	0.583	0.486	0.466
390	0.580	0.572	0.549

[a] Average value and standard deviation of B are 0.519 and 4.7%, respectively. [b] Results obtained by curve fitting using B and A_w or A_s as fitting parameters. [c] Results obtained by using a constant average B value and A_w or A_s as fitting parameters.

and are given in Table 2. From those values, linear relationships between A_w^2 or A_s^2 and Δt_n are obtained (Figure 4b, curves 3 and 4). From the slope of curve 3 and $B = 0.519$, $D_w = (1.31 \pm 0.06) \times 10^{-9}$ m^2 s^{-1} and $D_s^{eff} = (3.52 \pm 0.50) \times 10^{-10}$ m^2 s^{-1} were obtained in the liquid phase. From the slope of curve 4 in Figure 4 and $B = 0.519$, $D_w = (9.76 \pm 0.99) \times 10^{-10}$ m^2 s^{-1} and $D_s^{eff} = (2.63 \pm 0.04) \times 10^{-10}$ m^2 s^{-1} were obtained in the "solid" phase. The value of D_w calculated from the concentration profile in "solid" phase is lower than that in the liquid phase and closer to the literature value of 9.45×10^{-10} m^2 s^{-1}.[41] The larger value of D_w in the liquid phase (by ~30%) is probably due to small convective effects arising from unavoidable vibration (see also liquid−liquid interface), which do not occur in the "solid" phase. This is also suggested by the slight upward curvature of curve 3 (Figure 4b) which may be due to a slight increase of these convective effects with time. The overall validity of concentration gradients measured with IA-GIME is however confirmed by (i) the correct value of D_w measured in the "solid" phase, (ii) the similarity of the B values obtained in the liquid and "solid" phases, and (iii) the validity of the correction for porosity, tortuosity, and complexation in the "solid" phase. The latter is given by the ratio $[Pb^{2+}]/[Pb(II)]_t$, which can be computed (eq 15) from the data of Figure 4 as $[Pb^{2+}]/[Pb(II)]_t = FD_s^{eff}/D_w = 0.367$. This agrees very well with the value of 0.375 obtained from complexation measurements reported at the beginning of this section. All of these results demonstrate that reliable concentration in the solid phase can be determined from the slopes of calibration curves obtained in liquid phase even when effective diffusion coefficients in both phases are very different. This is linked to an important feature of gel-integrated microsensors (GIME), namely, the fact the gel is preequilibrated with the test medium before voltammetric measurements and the diffusion during voltammetric measurements only occurs inside the gel. Thus, current intensities measured on

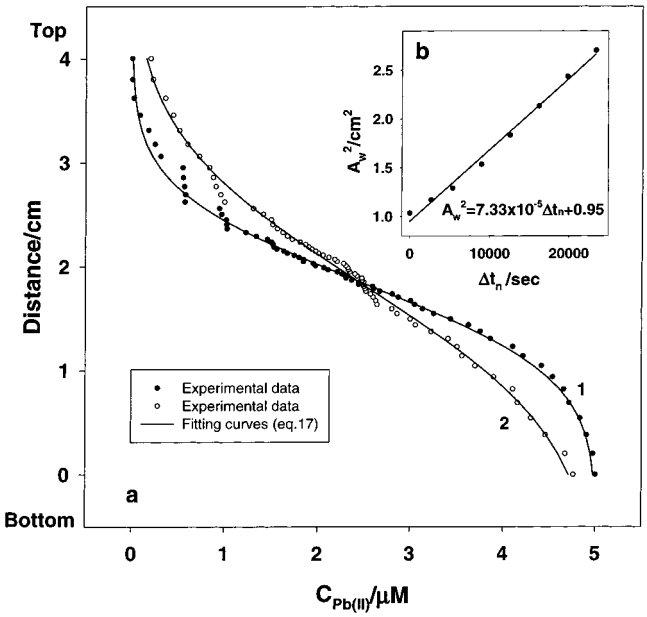

Figure 5. (a) Typical Pb(II) concentration gradients measured by SWASV at a liquid−liquid interface using the IA-GIME: (1) first measurements ($t = t_1$); (2) measurement 6.5 h later ($t = t_1 + 6.5$ h). Inset b, the linear relationship obtained between A_w^2 and Δt_n (see text). Solution composition used: top solution, 0.01 M $NaNO_3$ + 0.01 M acetate buffer solution (pH 4.5); bottom solution, 5 μM Pb(II) in 0.25 M $NaNO_3$ + 0.01 M acetate buffer solution (pH 4.5). SWASV conditions used as in Figure 2.

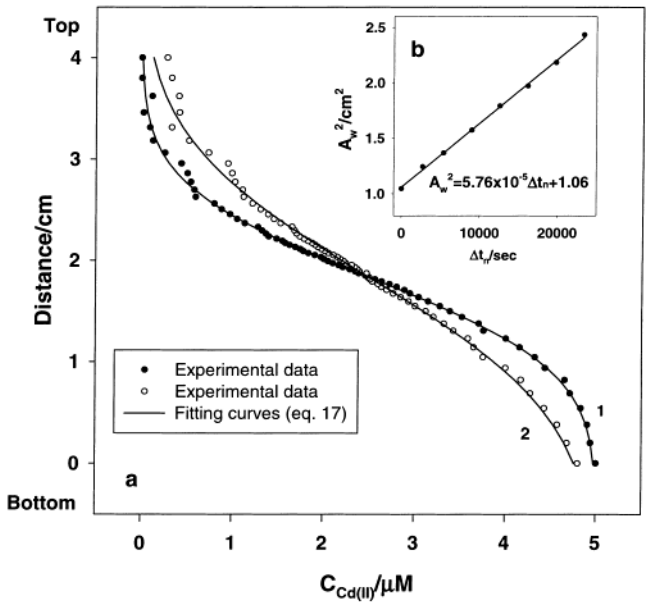

Figure 6. (a), Typical Cd(II) concentration gradient measured by SWASV at a liquid−liquid interface using the IA-GIME: (1) first measurement ($t = t_1$); (2) measurement 6.5 h later ($t = t_1 + 6.5$ h). Inset b, the linear relationship obtained between A_w^2 and Δt_n. Solution composition and SWASV conditions used as in Figure 5 except that Cd(II) (5 μM) was used instead of Pb(II).

the sensor lines are only a function of the diffusion in the gel and not in the external tested phases. This is a major advantage of GIME over more traditional voltammetric sensors (i.e., without the gel layer), as for these latter, the interpretation of current data measured in complex media in term of concentration is far from being straightforward.

Concentration Profile Measurements at a Well-Controlled Liquid−Liquid Interface. The profiling capability of the IA-GIME has been also tested by measuring Pb(II) and Cd(II) concentration gradients at a well-controlled liquid−liquid interface. The preparation of this interface is given in the Experimental Section. Pb(II) and Cd(II) are only added in the bottom layer, and they diffuse from the bottom to the top solution.

The concentration profiles of Pb(II) and Cd(II) were measured using SWASV. Typical curves are shown in Figure 5a and Figure 6a, respectively. For all the concentration profiles, the concentrations of Pb(II) and Cd(II) at the interface were ~2.5 μM, i.e., half of the initial concentration as expected from the theoretical equation applicable to both phases in this system:[40]

$$C(x,t) = \frac{1}{2}C_0 \operatorname{erfc}\frac{x}{2\sqrt{D_w t}} \qquad (16)$$

where x is the distance from the interface ($x > 0$ for the top layer and $x < 0$ for the bottom layer), t is the diffusion time, C_0 is the initial concentration of the diffusing substance, and D_w is the diffusion coefficient assumed to be equal in both phases. The experimental concentration profiles can be fitted with eq 16 rewritten as

$$C(z,t) = \frac{1}{2}C_0 \operatorname{erfc}\left(\frac{(z-d)}{A_w}\right) \qquad (17)$$

with $A_w = 2(D_w(t_1 + \Delta t_n))^{1/2}$, z is the distance from sensor line 1, d is the distance between sensor line 1 and the interface, and t_1 and Δt_n were the same meaning as in eqs 2a and 3a. Equation 17 was used because under our conditions, d and t_1 are not precisely known. As expected for a well-defined interface, a linear response was found between A_w^2 and Δt_n (Figure 5b and Figure 6b). The effective diffusion coefficients of Pb(II) and Cd(II), determined from the slopes of these curves, were found to be (1.83 ± 0.06) × 10^{-9} and (1.44 ± 0.03) × 10^{-9} m^2 s^{-1}, respectively. These values are ~2 times larger than the literature values for Pb(II) and Cd(II), which are 0.945 × 10^{-9} and 0.719 × 10^{-9} m^2 s^{-1}, respectively.[41] The standard deviations of d values for the eight Pb(II) and Cd(II) profile measurements (total duration, 6.5 h) were 1.2 and 1.5%, respectively, showing a well-defined interface, not significantly degraded by turbulences with time. The higher values of effective diffusion coefficients compared to the literature values may be due to several factors: (i) Due to the larger concentration of $NaNO_3$ in the bottom solution compared to the top solution, Na^+ and NO_3^- codiffuse with Pb(II) and Cd(II). Because of the larger mobility of NO_3^- (D = 1.9 × 10^{-9} m^2 cm^{-1}) compared to that of Na^+ (D = 1.37 × 10^{-9} m^2 cm^{-1}), an attractive effect on Pb(II) and Cd(II) may be produced, which may result in diffusion coefficients larger than one due to molecular diffusion only. This effect can be approximately corrected by considering the contribution of the electrical field of the coexisting ions. The diffusion coefficient, D_i, of an ion i codiffusing with ions j can be computed by eq 18:[48]

(48) Ben-Yaakov, S. *Geochim. Cosmochim. Acta* **1972**, *36*, 1395.

$$D_i = D_i^0 - D_i^0 z_i C_i \left[\frac{\sum_{j=1}^{n} z_j D_j^0 \left(\frac{dC_j/dx}{dC_i/dx} \right)}{\sum_{j=1}^{n} z_j^2 D_j^0 C_j} \right] \quad (18)$$

By applying eq 18 to our conditions, these computed diffusion coefficients of Pb(II) and Cd(II) are found to be 1.09×10^{-9} and 0.835×10^{-9} m^2 s^{-1}, respectively. The results show that the effect of codiffusion only increases the molecular diffusion coefficients by 15% in our case, which only explains a small part of the observed difference. (ii) The "natural" convection may influence the diffusional transport over a duration as long as 6.5 h despite the precaution used. This is confirmed by the fact that values of D_w similar to those in the literature are obtained at the more stable liquid− "solid" interface (see above). (iii) It is likely that some convection occurs at the interface during the introduction of the bottom solution while preparing the interface. This effect probably does not affact the slope of the curve $A^2 = f(\Delta t_n)$ very much. On the other hand, its existence is suggested by the too large value of t_1 (∼3.7 h) compared to the time really used (∼2.2 h) to introduce the bottom solution. All those considerations strongly suggest that some convection is the reason of the too large values of D_w observed here. It was out of the scope of this work to try to study this effect further. All results of the paper demonstrate that the IA-GIME is capable of providing reliable and useful concentration gradients under various physical and chemical conditions. The fact that it is sensitive to even weak convection effects is an additional advantage to study such effects.

CONCLUSION

This paper shows that the voltammetric IA-GIME and probe recently developed[30] allow accurate, real-time, high-spatial resolution concentration profile measurement at an interface with steep concentration gradients. In particular, it was demonstrated the following: (i) as peak current intensities measured using GIME area function of the diffusion coefficient in the gel only and not in the external tested media, slopes of calibration curves obtained in the synthetic liquid phase allow reliable determination of metal concentration in the solid phase; (ii) even small convective effects on the diffusion process can be detected; (iii) the effects of porosity, tortuosity, and complexation of the solid phase on the diffusion of analyte at a liquid−"solid" interface can be accurately measured with the IA-GIME. It is worth stressing that, in turn, interpretation of current data into concentration gradients implies a detailed knowledge of the above chemical and physical factors. This is a major aspect to consider for applications in more complicated biological or environmental systems. The results also show that the IA-GIME enables one to correctly follow the change of concentration profiles with time. This is a major advantage of the IA-GIME over single voltammetric microelectrodes and other techniques such as DGT and DET for real-time concentration profile measurements. Another advantage is that the geometry of this novel sensor can be readily modified and future miniaturization is possible to adapt to different types of applications. Thus, in addition to environmental applications, such a probe could be very useful in biological and biomedical applications, e.g., for gradient measurements around cells and tissue samples.

ACKNOWLEDGMENT

We acknowledge Mr. G. Riccardi, Mr. F. Confalonieri, Mr. A. Sina, and Mr. F. Graziottin (Idronaut Srl, Milan), who have developed the electronics and software of the voltammetric probe. We also thank Mr. David Kony for his help in using Matlab. This work was supported by the European Commission (MAS3-CT95-0033).

Received for review May 31, 2000. Accepted February 6, 2001.

AC000615E